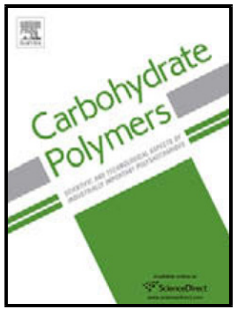


Title: A novel linear 3-O-methylated galactan isolated from *Cantharellus cibarius* activates macrophages

Authors: Guang Yang, Yunhe Qu, Yue Meng, Yushi Wang, Chengcheng Song, Hairong Cheng, Xiaomeng Li, Lin Sun, Yifa Zhou

PII: S0144-8617(19)30268-1
DOI: https://doi.org/10.1016/j.carbpol.2019.03.002
Reference: CARP 14671

To appear in:

Received date: 11 December 2018
Revised date: 18 February 2019
Accepted date: 3 March 2019

Please cite this article as: Yang G, Qu Y, Meng Y, Wang Y, Song C, Cheng H, Li X, Sun L, Zhou Y, A novel linear 3-O-methylated galactan isolated from *Cantharellus cibarius* activates macrophages, *Carbohydrate Polymers* (2019), https://doi.org/10.1016/j.carbpol.2019.03.002

# A novel linear 3-O-methylated galactan isolated from *Cantharellus cibarius* activates macrophages

Guang Yang, Yunhe Qu, Yue Meng, Yushi Wang, Chengcheng Song, Hairong Cheng, Xiaomeng Li, Lin Sun*, Yifa Zhou*

Jilin Province Key Laboratory on Chemistry and Biology of Changbai Mountain Natural Drugs, School of Life Sciences, Northeast Normal University, Changchun 130024, China

***Correspondence:**

Lin Sun, email: sunl925@nenu.edu.cn

Yifa Zhou, email: zhouyf383@nenu.edu.cn;

## Highlights

- A novel linear 3-O-methylated galactan (WCCP-N-b) from *C. cibarius* was identified.
- WCCP-N-b increased phagocytosis and secretion of NO, TNF-α, IL-6 and IL-1β.
- WCCP-N-b activated macrophages through Akt/NF-κB, MAPKs via TLR2 receptor.
- The molecular weight of WCCP-N-b impacted the activation.

**Abstract**

A novel polysaccharide (WCCP-N-b) with a molecular weight of 18 kDa was isolated and purified from the fruiting bodies of *Cantharellus cibarius*. Monosaccharide composition, methylation analysis and NMR spectra indicated that WCCP-N-b was a linear α-1,6-galactan, partially methylated at O-3 of galactose. The

molar ratio of Gal, 3-methylated-Gal, Glc and Man was 14.4:4.6:1.0:1.2. WCCP-N-b could significantly increase macrophage phagocytosis, release of NO and secretion of TNF-α, IL-6 and IL-1β. On a cellular mechanistic level, WCCP-N-b activated MAPKs and NF-κB signaling pathway via Toll-like receptor 2 (TLR2). To further elucidate the structure-function relationship, WCCP-N-b was hydrolyzed by acid. Four degraded fragments were obtained, with molecular weights of 16.1 kDa, 11.2 kDa, 5 kDa and 3.5 kDa, respectively. Their macrophage activation effects were significantly decreased along with the molecular weight decrease. Collectively, WCCP-N-b could activate RAW264.7 cells, and the activation effect was related to its molecular weight.

**Key words:** *Cantharellus cibarius*, Polysaccharide, 3-O-methylated galactan, Macrophage, TLR2

## 1. Introduction

Macrophages are important components of the innate immune system, playing a crucial role in host defense against infection trough immune-inflammatory responses, recognition of pathogens and phagocytosis. In addition, macrophages also exert an important role as an interface between innate and adaptive immunity (Van den Bossche, O'Neill & Menon, 2017). Hence, macrophages are thought to be the important target cells of some antitumor and immunomodulatory drugs. Many mushroom sugars that can bind to pattern recognition receptors (PRRs) such as TLR2, TLR4, Dectin-1 (Gordon, 2002) and stimulate immune system, which present on the surface of macrophage cells, and then activate MAPKs and NF-κB signaling pathway, induce the activation of immune response (Takeuchi & Akira, 2010).

Mushrooms are used as healthy food in the world as they are rich in a great variety of bioactive components, such as proteins (Zhang et al., 2014), lipopolysaccharides (Wasser, 2011), glycoproteins (Cui et al., 2013) and polysaccharides (Meng, Cheng, Han, Chen, & Wang, 2017). Among the bioactive compounds, polysaccharides are the most abundant and extensively studied. Polysaccharides from mushrooms possess antioxidant activity (Nowacka et al., 2014), antitumor activity (Wasser, 2002) and immunoregulatory activity (Meng, et al. 2018). These biologically active mushroom polysaccharides are mostly glucans (Liana et al., 2018) and galactans (Rosado et al., 2003) The main chains of the galactans are composed of (1→6)-linked α-D-Gal*p* units, which are partially methylated at O-3 or substituted at C-2 by L-fucopyranosyl, D-mannopyranosyl, D-galactopyranosyl or 3-O-α-D-mannopyranosyl-α-L-fucopyranosyl residues as side chains (Rosado et al.,

2003; Ruthes, Smiderle & Iacomini, 2016) have been reported, possess immunoregulatory activity.

*Cantharellus cibarius* (C. cibarius, the golden chanterelle) is an edible mushroom which widely distributes in Asia, America and some European countries. It belongs to the phylum Basidiomycota, family *Cantharel-laceae*. It is not only consumed as health-supplementary food, but also considered as adjuvant in improving eyesight and strengthening both spleen and stomach functions in traditional Chinese medicines (Wang, Ngai, & Ng, 2003; Han, et al., 2013). Polysaccharides, such as mannans (Nyman, Aachmann, Rise, Ballance, &Samuelsen, 2016) and glucans (Villares, et al., 2013; Zhao, et al., 2018) have been purified from *C. cibarius* fruit bodies. However, few studies about galactans from *C. cibarius* have been reported. In this paper, a novel galactan was isolated and purified from the fruit bodies of *C. cibarius*. The present study is aimed to study the structure of this galactan, evaluate its immunostimulatory activity on RAW264.7 cells, investigate the molecular mechanism responsible for its immunostimulatory activity, and illuminate its structure-activity relationship.

## 2. Materials and methods

### 2.1 Materials

Fruiting bodies of *C. cibarius* were purchased at the local market in Jilin Province, PR China and were identified by using rDNA-ITS sequencing analysis. DEAE-cellulose was purchased from Shanghai Chemical Reagent Research Institute (Shanghai, China). Sepharose CL-6B and Sephadex G-10 were purchased from GE

Healthcare (Little Chalfont, Buckinghamshire, UK). LPS was obtained from Sigma (Sigma Aldrich, St Louis, MO, USA). ELISA kits were obtained from Boster Biological Technology (Wuhan, China). LY294002, BAY11-7082, SP600125, U0126 and SB203580 were acquired from Selleck (Shanghai, China). TLR2 siRNA was obtained from JTSBIO (Wuhan, China). All of the other reagents were of analytical grade or better.

**2.2 Extraction and purification of the polysaccharide**

Fruiting bodies of *C. cibarius* were defatted with 95% ethanol (material/ethanol, w/v, 1:10), and the residues were first extracted with distilled water at 100 °C for 4 h (1:25w/v) followed by extracting again at 100 °C for 2 h (1:20 w/v). The extracts were concentrated under vacuum at 60 °C, and 95% ethanol was added at a final concentration of 65% to precipitate the polysaccharides. The precipitate was collected by centrifugation at 4000 rpm for 15 min and vacuum dried. A water-soluble polysaccharide named as WCCP with a yield of 5.5% (yield in relation to dry weight of initial material) was obtained. WCCP was dissolved in distilled water and centrifuged at 4000 rpm for 15 min. The supernatant was applied to a DEAE-Cellulose column ($Cl^-$, 1.5×14 cm) pre-equilibrated with distilled water. The column was first eluted with distilled water, yielding a neutral polysaccharide fraction (WCCP-N), and then eluted with 0.3 M NaCl to give an acidic fraction (WCCP-A). WCCP-N was further purified using gel-permeation chromatography with Sepharose Cl-6B to give a homogeneous fraction WCCP-N-b.

### 2.3 Analysis of chemical properties

Total carbohydrate content was determined by using the phenol-sulfuric acid protocol with glucose as the standard (Dubois, Gilles, Hamilton, Rebers, & Smith, 1951). Protein content was determined by using the Bradford assay with bovine serum albumin as the standard (Sedmak & Grossberg, 1977).

Monosaccharide composition was determined by using high performance liquid chromatography (HPLC) as described by Zhang (Zhang et al., 2009). Methyl-galactose (Me-Gal) was determined by UPLC-MS (Yan, et al., 2019).

Molecular weight distributions were determined by using high performance gel-permeation chromatography (HPGPC) on a TSK-gel G-3000PWXL column (7.8 × 300 mm, TOSOH, Japan) coupled to a Shimadzu HPLC system as described by Zhang et al. (2009). The column was pre-calibrated by using standard dextrans (50 kDa, 25 kDa, 12 kDa, 5 kDa and 1 kDa) using linear regression.

### 2.4 Acid hydrolysis of WCCP-N-b

WCCP-N-b (2 mg) was hydrolyzed with 1 ml TFA (1 M, 0.5 M, 0.25 M and 0.1 M) at 80 °C for 1 h, respectively, and then the aliquot was adjusted to pH 7 by adding 0.3 M NaOH. The hydrolysates were desalted by using Sephadex G-10 column and freeze dried.

### 2.5 Methylation analysis

Methylation analysis was carried out according to the method of Needs and

Selvendran (Needs & Selvendran, 1993). The partially methylated sugars in the hydrolysate were reduced by using $NaBH_4$ and acetylated (Sweet, Albersheim & Shapiro, 1975). The resulting alditol acetates were analyzed by GC-MS (7890B-5977B, Agilent, USA) with a HP-5ms capillary column (30 m × 0.32 mm × 0.25 mm). The oven temperature was programed from 120 °C (hold for 1 min) to 210 °C (hold for 2 min) at 3 °C/min, then up to 260 °C (hold for 4 min) at 10 °C/min. Both temperature of inlet and detector were 300 °C. Helium was used as carrier gas. The mass scan range was 50-500 m/z.

**2.6 NMR analyses**

Samples (20 mg) were dissolved in $D_2O$ (0.5 ml) and centrifuged to remove undissolved polysaccharide. $^{1}H$, $^{13}C$, HSQC, and HMBC NMR spectra were recorded at 20 °C on a Bruker Avance 600 MHz spectrometer (Germany) with a Bruker 5 mm broadband probe operating at 600 MHz for $^{1}H$ NMR and 150 MHz for $^{13}C$ NMR, respectively. Data were analyzed using standard Bruker software.

**2.7 Cell culture**

RAW264.7 cells were purchased from the American Type Culture Collection. RAW264.7 cells were maintained in DMEM high glucose medium supplemented with 100 U/ml penicillin, 100 μg/ml streptomycin and 10% heat-inactivated FBS. Cells were cultured at 37 °C in a 5% $CO_2$ incubator.

**2.8 Cell viability assay**

RAW264.7 cells were seeded at a density of $2\times10^5$ cells/ml in a 96-well plate

overnight and then treated with various concentrations of WCCP-N-b or 1 μg/ml of LPS for 24 h. Cell viability was determined by MTT assay (Meng, et al., 2018).

### 2.9 Measurement of NO

RAW264.7 cells at a density of $8\times10^5$/ml were incubated with different concentrations of WCCP-N-b or LPS (1 μg/ml) for 24 h. After incubation, supernatants were collected and reacted with Griess reagent (Meng, et al., 2018).

### 2.10 Determination of phagocytic uptake capacity of macrophage

RAW264.7 cells were seeded at a density of $4\times10^5$/well in 6-well plate overnight and incubated with different concentrations of WCCP-N-b or LPS (1 μg/ml) for 24 h. The phagocytic activity of macrophages was analyzed using flow cytometry (Yan, et al., 2018). The phagocytosis index was calculated as the number of phagocytosed beads/total number of macrophages.

### 2.11 Measurement of TNF-α, IL-6 and IL-1β

RAW264.7 cells were pretreated with or without specific inhibitors (25 μM of SB203580, 25 μM of U0126, 20 μM of SP600125, 25 μM of LY294002, 10 μM of BAY11-7082) for 2 h, followed by incubation with WCCP-N-b (200 μg/ml) for 24 h. The concentrations of TNF-α, IL-6 and IL-1β were assessed using ELISA kits according to the manufacturer's instructions.

### 2.12 Antibody inhibition experiments

Cells were pretreated with function-blocking antibodies (20 μg/ml each) to TLR2, TLR4, Dectin-1 for 2 h, followed by incubation with WCCP-N-b for 24 h. Cytokine

concentration was examined using ELISA kits according to the manufacturer's instruction.

**2.13 Immunofluorescence assay**

Macrophages were fixed in 4% paraformaldehyde for 30 min and incubated with anti-NF-κB p65 antibody (1:200) for 1 h at room temperature. Then cells were washed three times with PBS and incubated with FITC secondary antibody (1:200) for 1 h at room temperature. Nucleus was stained with Hoechst reagent for 10 min at room temperature. The location of NF-κB p65 was assessed using immunofluorescence microscopy.

**2.14 Western blotting**

WCCP-N-b (200 μg/ml) was added to each well ($8\times10^5$ cells) and maintain at 37 ℃ for 30 min. The Western blotting assay was performed as previously described (Meng, et al. 2018).

**2.15 Transfection**

Transfection of RAW264.7 cells was conducted with Lipofectamine 3000 (Thermo Fisher Scientific, USA) following the manufacturer's instructions. High purity controls (scrambled RNA), along with TLR2 siRNA oligos, were obtained from JTSBIO (Wuhan, China). The targeting sequences of the siRNA constructs are: TLR2 siRNA-1, 5'-GCCUUGACCUGUCUUUCAATT-3'; TLR2 siRNA-2, 5'-CCAGCAGAAUCAAUACAAUTT-3'. After 48 h of transfection, RAW264.7 cells were treated with WCCP-N-b (200 μg/ml) for 30 min or 24 h, and then analyzed by western blotting or ELISA assay, respectively.

### 2.16 Statistical analysis

Data are provided as the mean ± SD from at least three independent experiments. Differences between the groups were analyzed through a one-way analysis of variance (ANOVA). Significance was defined as *P*-values < 0.05, 0.01 or 0.001, respectively.

## 3. Results

### 3.1 Extraction and purification of polysaccharide from *Cantharellus cibarius*

The water-soluble polysaccharide (WCCP) was extracted from the fruiting bodies of *C. cibarius* (Fig. 1A), with a yield of 5.5% in relation to dry weight of initial material. WCCP was fractionated by ion-exchange chromatography into a neutral polysaccharide fraction WCCP-N (yield 50.2%) and an acid polysaccharide fraction WCCP-A (yield 29.2%) (Fig. 1B). WCCP-N was further purified with gel permeation chromatography and a major homogeneous fraction WCCP-N-b was obtained (Fig. 1C). The molecular weight of WCCP-N-b was around 18.0 kDa determined by HPGPC (Fig. 1D). Monosaccharide composition analysis showed that WCCP-N-b contained galactose (Gal) and 3-methyl-Gal as the main component, followed by minor of glucose (Glc) and mannose (Man), with the molar ratio of 14.4:4.6:1.0:1.2 (Table 4), respectively.

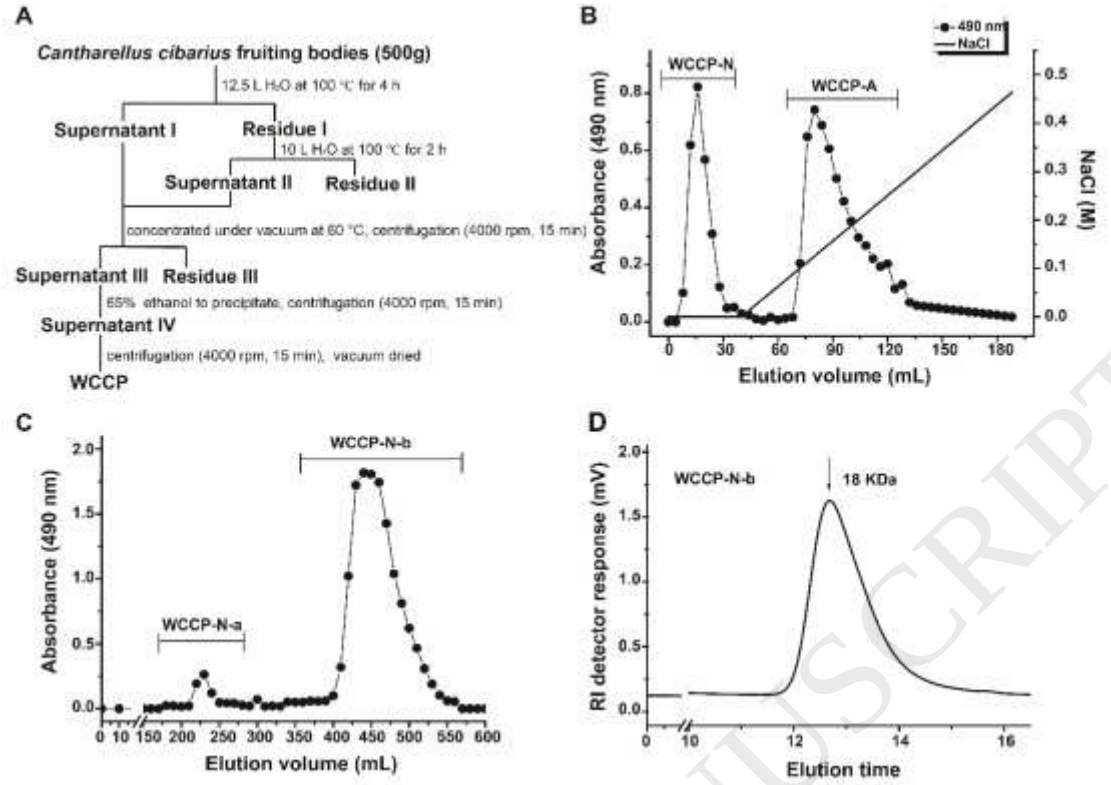


**Fig. 1. Extraction and purification of polysaccharides.** (A) Extraction scheme of water-soluble polysaccharide (WCCP) from *C. cibarius*. (B) WCCP was separated by DEAE-cellulose anion-exchange chromatography to give WCCP-N and WCCP-A. (C) WCCP-N was purified by Sepharose Cl-6B column to give WCCP-N-b. (D) Elution profile of WCCP-N-b on HPGPC.

### 3.2 Methylation analysis

In order to determine the glycosyl linkage types of WCCP-N-b, it was methylated, hydrolyzed and acetylated, and the partially methylated alditol acetates were analyzed by GC-MS. The methylation analysis result (Table 1) indicated that major glycosyl linkage type in WCCP-N-b was 1,6-linked-Gal*p* (including 1,6-linked-Me-Gal*p*), with the molar ratio of 91.1%. Small amounts of 1,2,6-linked-Gal*p* were also detected (3.2%). Therefore, the backbone of WCCP-N-b should be 1,6-linked-Gal*p*. The

degree of branching (DB) was only 3.4%. Trace amounts of 1,6-linked-Glc*p* (2.9%) and non-reducing terminals Man*p* (2.7%) were found. According to these results, the backbone of WCCP-N-b was composed of around one hundred Gal residues., among which around three Gal residues in the backbone were substituted at C-2 by very short branches.

**Table.1.** Linkage type analysis of WCCP-N-b by GC-MS

| Metylated sugars | Linkages | Molar ratio (mol %) | Mass fragments (m/z) |
|---|---|---|---|
| 2,3,4-$Me_3$-Gal*p* | 1,6- | 91.1 | 87,101,117,129,161,173,189,233 |
| 3,4-$Me_2$-Gal*p* | 1,2,6- | 3.2 | 87,99,117,129,159, 189,233 |
| 2,3,4-$Me_3$-Glc*p* | 1,6- | 2.9 | 87,101,117,129,161,173,189,233 |
| 2,3,4,6-$Me_4$-Man*p* | 1- | 2.7 | 87,101,117,129,145,161,205 |

**3.3 NMR analysis.**

The structure of WCCP-N-b was further characterized by 1D/2D NMR spectra. In the $^{1}$H-NMR spectrum, the signal at 4.93 ppm was assigned to H-1 of α-1,6-linked D-Gal*p* and 3-O-Me-D-Gal*p* residues (Zhang, Xu, Fu & Sun, 2013). The signal at 3.37 ppm was assigned to proton of O-$CH_3$ group (Ruthes et al., 2013) (Fig. 4A). No obvious signals for Glc*p* and Man*p* residues were detected since their quite lower content. In the $^{13}$C-NMR spectrum, signals at 97.61 ppm and 97.55 ppm were assigned to anomeric carbons of 1,6-linked Gal*p* and 3-O-Me-Gal*p*, respectively. Weak signal peak at 98.19 ppm was attributed to 1,2,6-linked Gal*p*. The signal at 78.56 ppm was corresponded to C-3 of α-1,6-linked 3-O-Me-D-Gal*p* (Cho, Yun, Yoo & Koshino, 2011). The signal at 55.88 ppm was assigned to carbon of O-$CH_3$ group (Fig. 4B). No obvious signal of C-2 for 1,2,6-linked α-D-Gal*p* was detected in the

$^{13}$C-NMR spectrum, which was consistent with methylation analysis result that quite lower content (3.2%) of 1,2,6-linked Gal*p* was determined. The other chemical shifts were assigned mainly according to carbon and hydrogen correlations in the HSQC (Fig. 4C) and HMBC spectra (Fig. 4D). On the basis of the proton assignments, the chemical shifts of H-1/C-1~H-6/C-6 for Gal*p* and 3-O-Me-Gal*p* were readily obtained from the HSQC spectrum (Carbonero et al., 2008). The sequence of the major residues in the repeating unit was identified from the HMBC spectrum, which showed clear correlations: **A**C-1/**B**H-6a/6b; **A**H-1/**A**C5; **B**C-1/**A**H-6a/6b; **B**H-1/**B**C-5; **O-CH$_3$**H-**B**C3; **O-CH$_3$**C-**B**H3. In conclusion, the possible structural feature of WCCP-N-b was proposed as a linear methylated galactan which was composed of α-1,6-linked D-Gal and 3-O-Me-D-Gal residues. This structure has never been reported in *C. cibarius.*

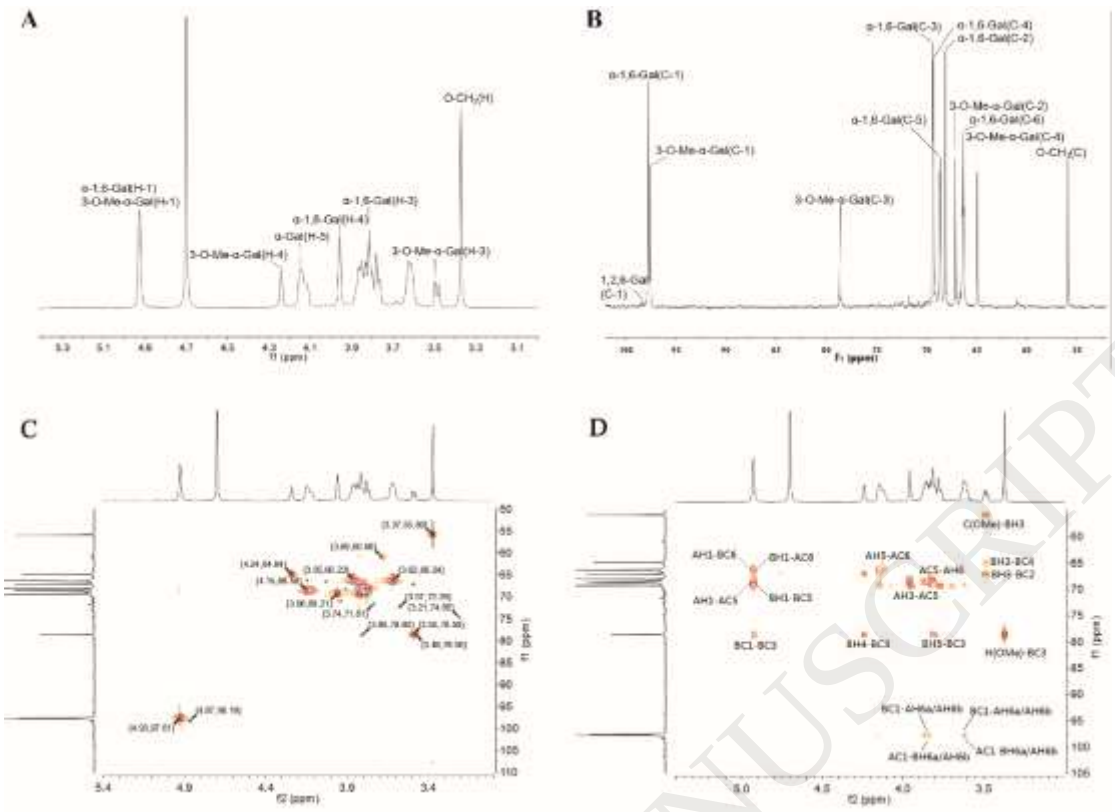


**Fig. 2. NMR spectra of WCCP-N-b.** (A) $^{1}H$ NMR spectrum, (B) $^{13}C$ NMR spectrum, (C) HSQC spectrum, (D) HMBC spectrum.

**Table 2.** HSQC spectral assignments for WCCP-N-b.

| Linkage type | | 1 | 2 | 3 | 4 | 5 | 6 | O-$CH_3$ |
|---|---|---|---|---|---|---|---|---|
| (A)α-1,6-D-3-Me-Gal*p* | H | 4.93 | 3.80 | 3.50 | 4.24 | 4.15 | 3.85;3.62 | 3.37 |
| | C | 97.55 | 67.06 | 78.56 | 64.84 | 68.67 | 66.24 | 55.88 |
| (B) α-1,6-D-Gal*p* | H | 4.93 | 3.78 | 3.81 | 3.96 | 4.15 | 3.85;3.62 | -- |
| | C | 97.61 | 68.02 | 69.31 | 69.21 | 68.60 | 66.24 | -- |
| (C) α-1,2,6-D-Gal*p* | H | 4.87 | 3.80 | 3.78 | 3.96 | 4.15 | 3.86;3.62 | -- |
| | C | 98.19 | 78.60 | 69.38 | 69.21 | 68.58 | 64.83 | -- |

**Table 3.** HMBC spectral assignments for WCCP-N-b

| Glycosidic linkage | H-3/C-3 | H-1/C-1 | Coupling relationship | | |
|---|---|---|---|---|---|
| | | | $\delta_H/\delta_C$ | Residue | Atom |
| (C)α-1,6-D-3-Me-Gal*p* | | 4.93 | 66.24 | D | C6 |
| | | | 68.54 | C | C5 |
| | | | 78.56 | C | C3 |
| | 3.50 | | 55.80 | O-$CH_3$ | Me(C) |
| | 78.56 | | 3.37 | O-$CH_3$ | Me(H) |
| | | 97.55 | 3.86 | D | H6a |
| | | | 3.62 | D | H6b |
| (D)α-1,6-D-Gal*p* | | 4.93 | 66.24 | C | C6 |
| | | | 68.58 | D | C5 |
| | | 97.71 | 3.85 | C | H6a |
| | | | 3.62 | C | H6b |

### 3.4 WCCP-N-b promotes activation of macrophages.

The cytotoxicity effect of WCCP-N-b on RAW264.7 macrophage cells was investigated by the MTT assay. Results showed that WCCP-N-b minimally affect cell viability (Fig. 3A), indicating the absence of cytotoxic effects. Macrophage activation was assessed by assessing release of NO, phagocytic uptake and secretion of the cytokines (TNF-α, IL-6, IL-1β). LPS was applied as a positive control. Compared to

the control group, WCCP-N-b significantly induced production of NO (Fig. 3B), obviously increased phagocytic uptake (Fig. 3C), as well as robustly provoked the secretion of TNF-α, IL-6 and IL-1β (Fig. 3D).

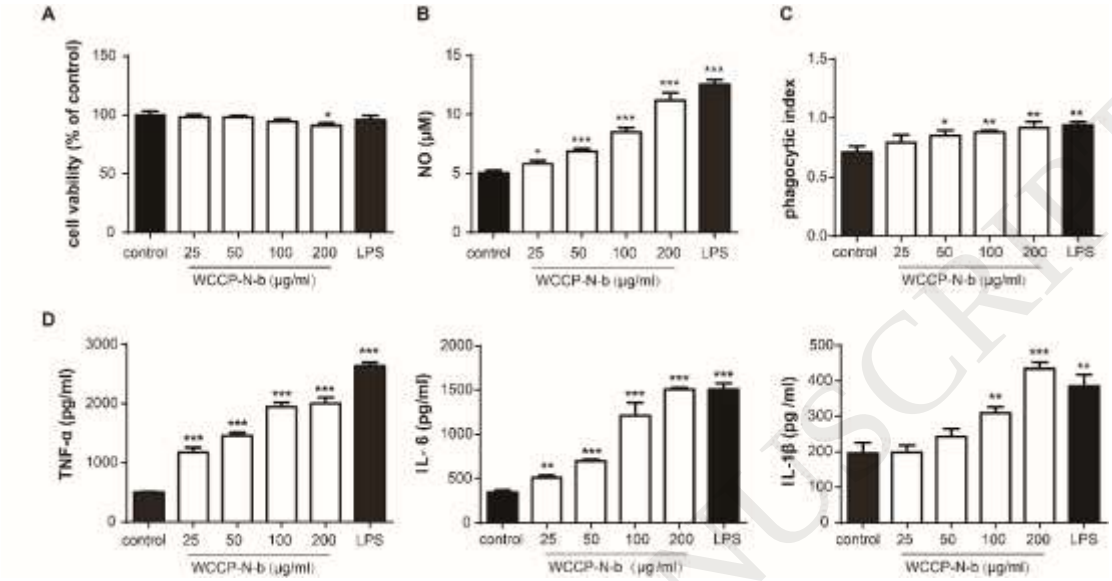


**Fig. 3. WCCP-N-b promoted the activation of RAW264.7 cells.** RAW264.7 cells were treated with the indicated doses of WCCP-N-b for 24 h. (A) Cell viability was determined by MTT assay. (B) Releases of NO was analyzed with Griess reagents. (C) Phagocytic uptake was assessed by determining the uptake of fluorescent microspheres using flow cytometry. (D) Secretion of the cytokines TNF-α, IL-6 and IL-1β was examined using the ELISA assay. Error bars in (A), (B), (C), and (D) represent the S.D. (N = 3 independent experiments). **P*< 0.05, ** *P*< 0.01 and ****P*< 0.001, compared to control group.

### 3.5 MAPK pathway is related to RAW264.7 activation.

Mitogen-activated protein kinases (MAPKs), including the extracellular signal-regulated kinases (ERKs), c-Jun N-terminal kinases (JNKs), and p38-MAPKs, have been reported to be involved in macrophage activation (Meng et al., 2018). In the present study, whether MAPK pathway was involved in the WCCP-N-b-induced

macrophage activation was investigated. The results showed that WCCP-N-b increased phosphorylation of ERK, JNK and p38 (Fig. 4A). Pre-treatment cells with ERK inhibitor U0126, JNK inhibitor SP600125 or p38 inhibitor SB203580 significantly reduced the phosphorylation of ERK, JNK and p38, respectively. Furthermore, secretion of NO, as well as TNF-α and IL-6 production, were also significantly reduced (Fig. 4C). Taken together, we concluded that MAPK pathway accounted for, at least partially, the macrophage activation by WCCP-N-b.

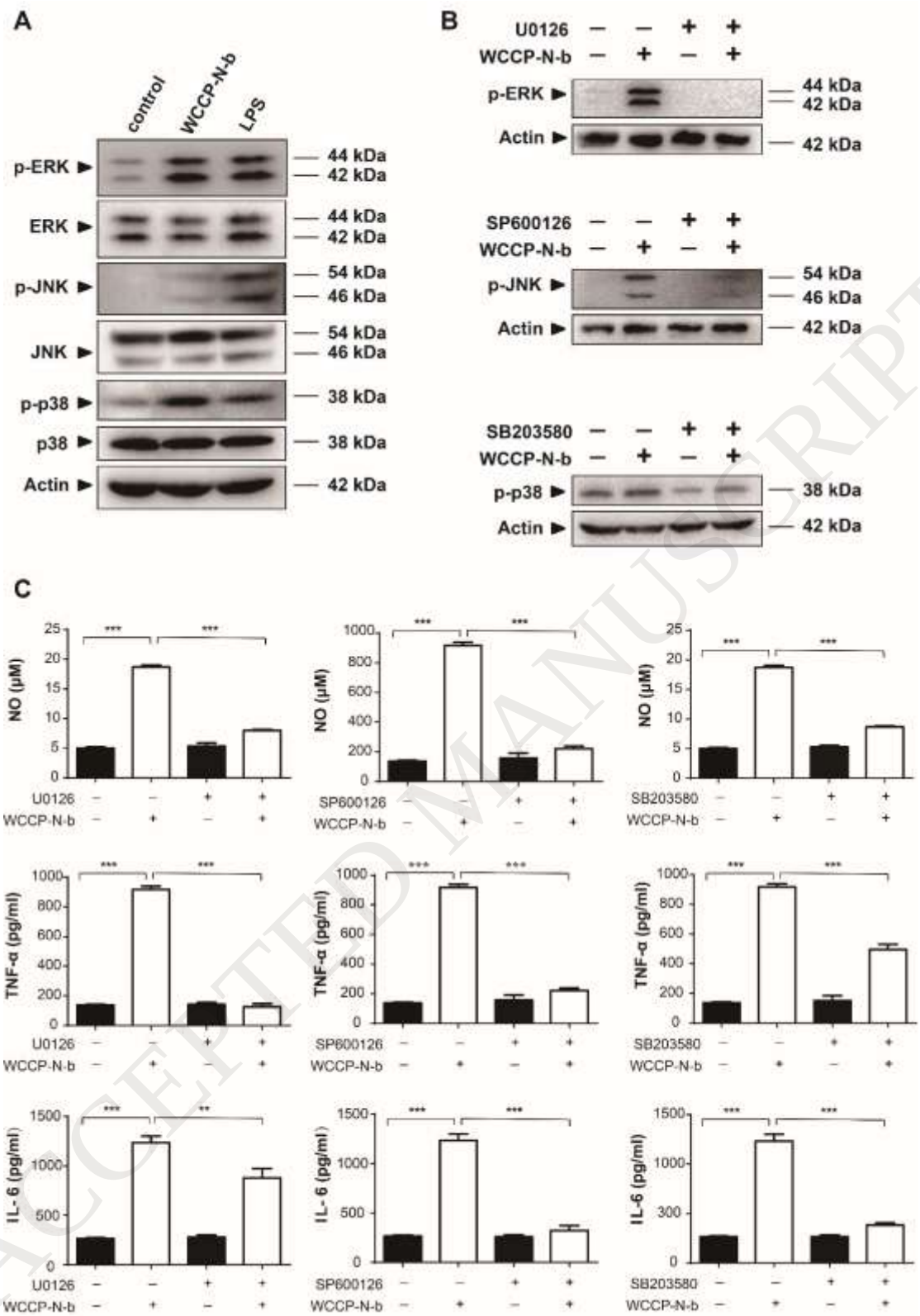


**Fig. 4. Effect of WCCP-N-b on MAPKs signaling pathways.** RAW264.7 cells were treated with 200 μg/ml of WCCP-N-b for the indicated concentrations for 30 min (A). RAW 264.7 cells were pretreated with or without the ERK inhibitor U0126, the JNK inhibitor SP600126 and the p38 inhibitor SB203580 for 2 h, followed by incubation

with WCCP-N-b (200 μg/ml) or LPS (1 μg/ml) for 30 min (B). Whole-cell extracts were analyzed by western bolt. (C) RAW264.7 cells were treated with 200 μg/ml of WCCP-N-b for 24 h, NO production, TNF-α and IL-6 secretion were detected by using Griess reagents and ELISA assay, respectively. Error bars in (C) represent the S.D. (N= 3 independent experiments). $^{**}P< 0.01$ and $^{***}P < 0.001$.

### 3.6 WCCP-N-b induces AKT/NF-κB activation in RAW264.7 cells.

The nuclear factor κB (NF-κB) signaling pathway is essential for regulation of a wide variety of cellular genes, especially those involved in immune and inflammatory responses (Cao, Li, Chen, Xue, & Liu, 2016). In resting cells, inactive NF-κB forms a complex with IκB-α and exists as a latent form in the cytosol. However, upon stimulation, IκB-α in the cytosolic complex is phosphorylated and degraded, which results in release of NF-κB and translocation to the nucleus allowing NF-κB to interact with its promoter elements and mediate transcription of a variety of target genes (Yan, et al., 2018). It has been reported that Akt activation is the upstream of NF-κB activity (Cianciulli et al., 2016). In the present study, immunofluorescence assay results showed that most cytoplasmic NF-κB p65 translocated from the cytoplasm to the nucleus when cells were treated with WCCP-N-b (Fig. 5A). Western blot analysis indicated that WCCP-N-b increased phosphorylation of AKT, degradation of IκB-α as well as phosphorylation of NF-κB (Fig. 5B). To validate the roles of AKT and NF-κB, inhibitor LY294002 to AKT and inhibitor BAY11-7082 to NF-κB were applied. The results showed that NF-κB inhibitor BAY11-7082 significantly reduced NF-κB phosphorylation (Fig. 5C). AKT inhibitor significantly

reduced phosphorylation of AKT, and subsequent IκB-α degradation as well as NF-κB phosphorylation (Fig. 5C). In addition, the secretion of NO, TNF-α and IL-6 were also robustly inhibited upon pretreatment of LY294002 or BAY11-7082 (Fig. 5D). Overall, these results indicated that the AKT/NF-κB signaling pathway is also involved in WCCP-N-b-induced activation of macrophages.

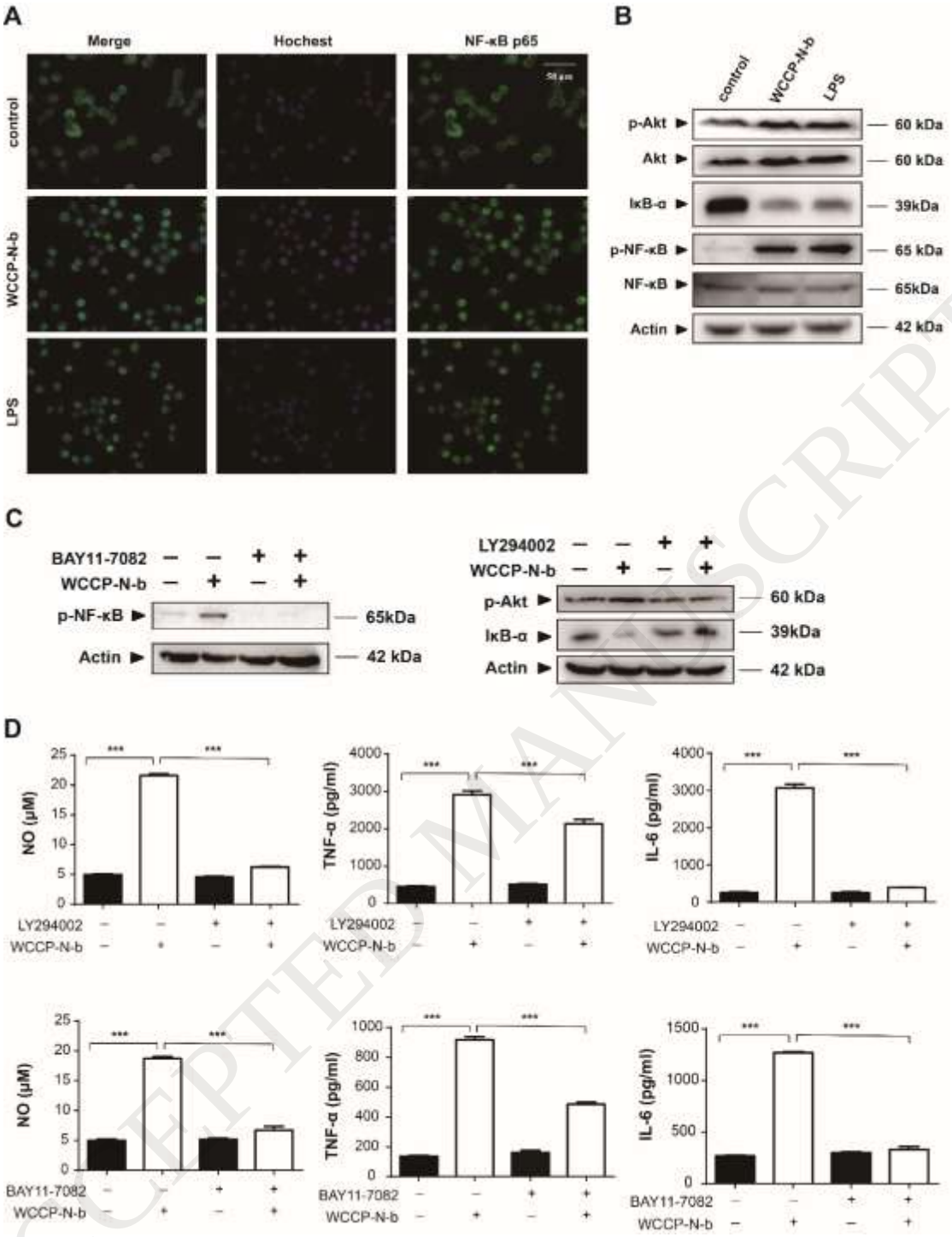


**Fig. 5. Effect of WCCP-N-b on NF-κB signaling pathways.** (A) The localization of NF-κB subunit (green) and nucleus (blue) were analyzed by double immunofluorescence staining following treatment with WCCP-N-b for 30 min. (B) RAW264.7 cells were treated with 200 μg/ml of WCCP-N-b for the indicated concentrations for 30 min, whole-cell extracts were prepared and analyzed by western

blotting. RAW 264.7 cells were pretreated with or without the AKT inhibitor (LY294002) or the NF-κB inhibitor (BAY11-7082) for 2 h, (C) followed by incubation with WCCP-N-b (200 μg/ml) for 30 min. Whole-cell extracts were analyzed by western bolt. (D) RAW 264.7 cells were pretreated with or without the AKT inhibitor (LY294002) or the NF-κB inhibitor (BAY11-7082) for 2 h, then treated with 200 μg/ml of WCCP-N-b for 24 h. NO production, TNF-α and IL-6 secretion were detected by using Griess reagents and ELISA assay, respectively. Error bars in (D) represent the S.D. (N= 3 independent experiments). ***$P$< 0.001.

### 3.7 Knockdown of TLR2 in RAW264.7 cells suppresses WCCP-N-b-induced macrophage activation

Polysaccharides cannot penetrate cells directly, because of their relatively large molecular mass. Therefore, polysaccharides need to bind to cell membrane receptors in order to mediate intracellular events and thereby trigger an immune response. Several pattern recognition receptors (PRRs), including TLR2, TLR4 and Dectin-1, have been reported to participate in signal transmission and thereby macrophage activation (Gordon, 2002). To determine which PRR participate in WCCP-N-b-induced macrophage activation, function-blocking antibodies of Dectin-1, TLR2 or TLR4 were applied. We found that only the anti-TLR2 antibody could abrogate WCCP-N-b-induced TNF-α and IL-6 cytokine release (Fig. 6A). To further confirm the role of TLR2, we transfected RAW264.7 cells with TLR2 siRNA. Compared with scrambled RNA group, TLR2-siRNA1 and 2 significantly decreased TLR2 expression (Fig. 6B). Moreover, WCCP-N-b-induced production of NO, TNF-α

and IL-6 were significantly inhibited in TLR2 siRNA transfected cells (Fig. 6C). These data indicated that TLR2 plays a vital regulatory role in the macrophage activation induced by WCCP-N-b.

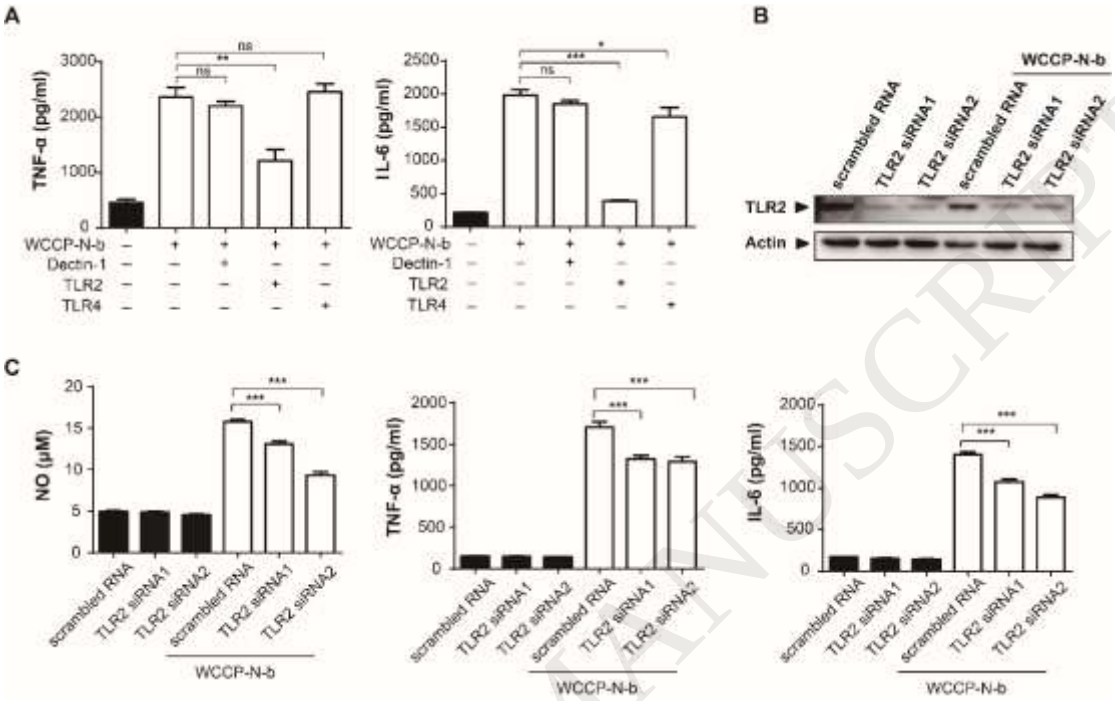


**Fig. 6. WCCP-N-b activated RAW264.7 cell via TLR2 receptor.** (A) RAW 264.7 cells were pretreated with or without function-blocking antibodies (20 μg/ml each) to Dectin-1, TLR2, TLR4 for 2 h, followed by incubation with WCCP-N-b (200 μg/ml) for 24 h. The production of TNF-α and IL-6 in the supernatants were determined by ELISA assay. RAW264.7 cells were transfected with scrambled RNA or TLR2 siRNA, and then treated with WCCP-N-b (200 μg/ml) for 30 min or 24 h. Protein expressions were detected by western blot (B). NO production or secretion of TNF-α and IL-6 in the culture supernatant were measured by the Griess assay (B) or ELISA assay (C), respectively. Error bars in represent the S.D. (N =3 independent experiments). **P*< 0.05, ***P* < 0.01 and ****P* < 0.001, ns, no significance.

### 3.8 Molecular weight of WCCP-N-b plays critical role on its macrophage activation effect

To further elucidate the structure-function relationship, WCCP-N-b was treated with 0.1 M, 0.25 M, 0.5 M and 1.0 M TFA solutions, respectively. A series of degraded fragments were obtained, named as WCCP-N-b1 (yield 60%), WCCP-N-b2 (yield 54%), WCCP-N-b3 (yield 37.8%) and WCCP-N-b4 (yield 33.8%). Their molecular weights were 16.1 kDa, 11.2 kDa, 5 kDa and 3.5 kDa, respectively (Fig. 7A). Compared with WCCP-N-b (molecular weight of 18 kDa), their molecular weights were all decreased. The monosaccharide composition of these degraded fragments (WCCP-N-b1~WCCP-N-b4) were similar to that of WCCP-N-b (Fig. 7B, Table 4.). Immunological activity analyses showed that the macrophage activation effects of these degraded polysaccharide fragments were significantly weaker than that of WCCP-N-b. The lower the molecular weight, the weaker the macrophage activation effect (Fig. 7C, D and E). Furthermore, we noted that when the molecular weight was decreased to 3.5 kDa, the polysaccharide fragment could not induce the secretion of NO, TNF-α and IL-6 (Fig. 7C, D and E). Therefore, we speculated that molecular weight of WCCP-N-b plays a crucial role inactivation of macrophages.

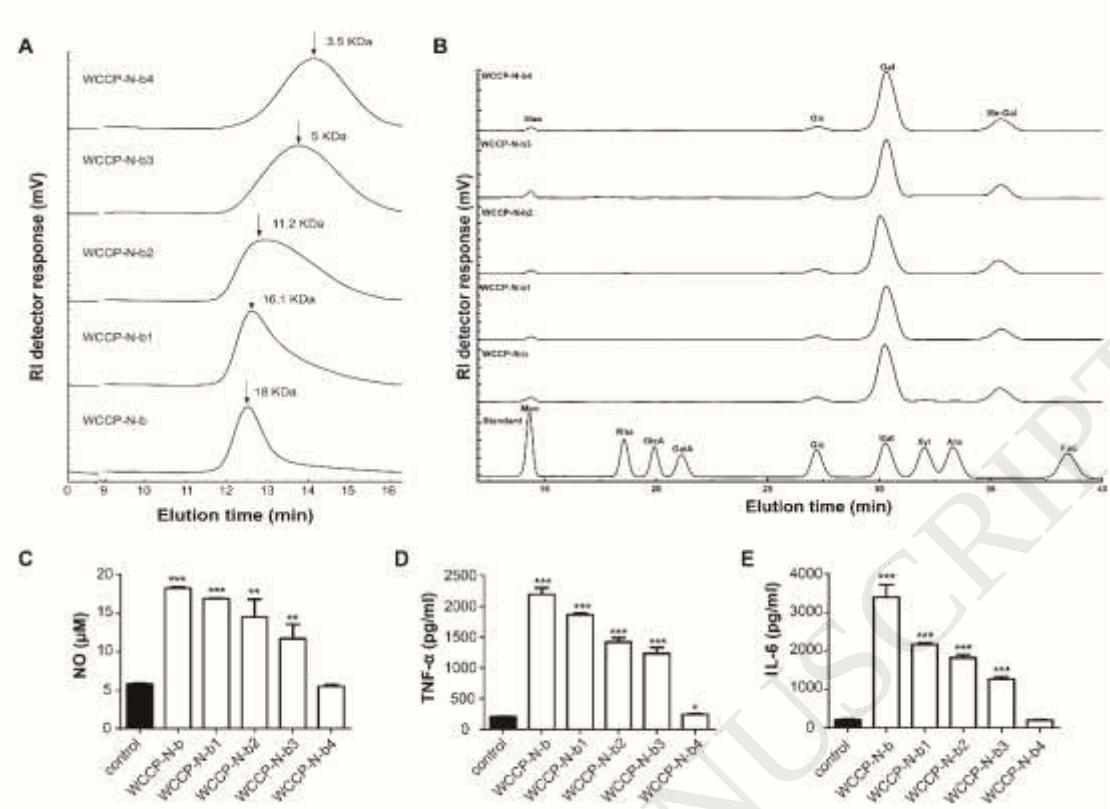


**Fig. 7. Molecular weight of WCCP-N-b affected the activation of macrophages.** (A) Molecular weight distribution of WCCP-N-b, WCCP-N-b1, WCCP-N-b2, WCCP-N-b3, WCCP-N-b4. (B) Monosaccharide composition analysis of WCCP-N-b, WCCP-N-b1, WCCP-N-b2, WCCP-N-b3, WCCP-N-b4 by HPLC, and the peak of Me-Gal appeared in 36min was confirmed by LC-MS analysis (Yan, et al., 2019). RAW264.7 cells were treated with polysaccharides (200 μg/ml) for 24 h, release of NO was analyzed by using Griess reagents (C), secretion of TNF-α and IL-6 were examined using the ELISA assay (D & E). Error bars represent the S.D. (N = 3 independent experiments). *$P$< 0.05, ** $P$ < 0.01and***$P$ < 0.001 compared to control group.

**Table 4.** Yield and monosaccharide composition of collected fractions

| Fraction | Yield (g%) [a] | Monosaccharide composition (%) | | | |
|---|---|---|---|---|---|
| | | Gal | Me-Gal | Man | Glc |
| WCCP-N-b | -- | 67.9 | 21.8 | 5.5 | 4.7 |
| WCCP-N-b1 | 60 | 67.8 | 23.0 | 6.2 | 3.0 |
| WCCP-N-b2 | 54 | 66.6 | 22.1 | 6.8 | 4.5 |
| WCCP-N-b3 | 37.8 | 67.5 | 21.5 | 5.4 | 5.6 |
| WCCP-N-b4 | 33.8 | 66.5 | 22.0 | 6.0 | 5.5 |

[a]Yield in relation to fraction WCCP-N-b

## 4. Discussion

*Cantharellus cibarius* is an edible mushroom widely used as healthy food in the world. Polysaccharide is one of the major components in *C. cibarius*. Lemieszek, Nunes, Cardoso, Marques, & Rzeski, (2018) isolated four polysaccharide fractions from *C. cibarius* fruit bodies, and these fractions were all made up of Man in the form of 1,6- and 1,4-linkages, with Glu and Fuc branches. Nyman, et al. (2016) purified three polysaccharide fractions from *C. cibarius* which were branched (1 → 6)-α-mannan and β-glucans. Two D-Glc*p* polysaccharides were isolated from *C. cibarius* by Villares, et al. (2013). Zhao, et al., (2018) purified a 1,4-linked-β-D-glucose which branched by α-D-xylopyranose residue at O-6 from *C. cibarius* fruit bodies. In the present study, we obtained a novel linear 3-O-methylated galactan (WCCP-N-b) from *C. cibarius*, which was composed of 67% of α-1,6-D-Gal*p* and 22% of α-1,6-D-Me-Gal*p*. The structure of WCCP-N-b was completely different from those polysaccharides above-mentioned. To our knowledge, this polysaccharide structure has not been reported in *C. cibarius*.

Mushrooms have been used both as food and medicine for last few decades.

Polysaccharide, as the main active ingredient in mushroom, has attracted much attention. Polysaccharides from mushrooms possess immunoregulatory activity. In most cases, polysaccharides cannot enter cells directly. A lot of evidences showed that the first step for polysaccharides to exert any function on cells was the recognition by PRRs (Yan, et al., 2018). A heterogalactan which consisted of a (1,4)-Gal*p* and (1,4)-GalA*p* backbone activated NF-κB signaling pathway, induced macrophages to release TNF-α *via* bingding to TLR4 （Wang, H. T., et al., 2018）. Meng, et al. (2018) isolated an α-(1,6)-D-galactan which was branched at the O-2 of Gal*p* residues by α-D-(1,6)-linked Man*p* attached to t-β-D-Glc*p* or t-α-D-Fuc*p* side chains from *Flammulina velutipes*, activated macrophage via TLR4 receptor. Yan, et al., (2019) extracted a partially 3-O-methylated galactans (WPEP-N-b) from *Pleurotus eryngii* which was composed of α-1,6-D-Gal*p* and α-1,6-D-3-O-Me-Gal*p* as main chains, branched at O-2 with single t-β-D-Man*p* as major side chain, could bind to TLR2 to activate macrophage. In the present study, the linear 3-O-methylated galactan WCCP-N-b could also activate MAPKs and NF-κB signaling pathway via TLR2 to promote immune activity. We speculated the galactan structure lead to its ability to bind to Toll-like receptor and heterogalactan partially substituted at O-3 by methyl groups might play a crucial role on its specific recogonization to TLR2. TLR2 could mediate activation of macrophage, B cells (Han et al., 2003), human monocytes (Balachandran, Pugh, Ma, & Pasco, 2006), NK cells (Ke, et al., 2014). Hence, we speculated that our 3-O-methylated galactan might be a promising and broad immunopotentiator via binding to TLR-2 receptor. Studies on the role of O-3 methyl

groups in the binding to TLR2 are ongoing in our laboratory.

In the present research, we found that the macrophage activation effect of galactan was decreased following with the decrease of the molecular weights of the galactan during acid hydrolysis. When the molecular weight was decreased to 3.5 kDa, the polysaccharide fragment could not induce the secretion of NO, TNF-α and IL-6. We speculated that the binding of the galactan to TLR2 was correlation with its spatial structure. However, further studies are needed to substantiate this hypothesis.

## 5. Conclusion

WCCP-N-b, the polysaccharide purified from the fruiting bodies of *Cantharellus cibarius*, was a linear galactans composed of 67% of α-1,6-D-Gal*p* and 22% of α-1,6-D-Me-Gal*p*. Immunomodulatory activity analysis showed that WCCP-N-b significantly activated RAW264.7 macrophages through increasing phagocytic uptake and inducing secretion of NO, TNF-α, IL-6 and IL-1β. On a cellular mechanistic level, WCCP-N-b activated MAPK/NF-kB signaling pathways via TLR2 receptor. The molecular weight of WCCP-N-b played a critical role on its macrophage activation effect.

## Acknowledgements

This work was supported by the National Natural Science Foundation of China (No: 31500274, 31770852), the University S & T Innovation Platform of Jilin Province for Economic Fungi (#2014B-1) and Natural Science Foundation of Changchun City of China (17DY026).

## Author Contributions

Y. Zhou conceived the study and revised the manuscript. G. Yang performed the activities and mechanisms research of the polysaccharide and drafted the manuscript. Y. Qu performed the polysaccharide extraction, isolation and purification. Y. Meng and Y. Wang repeated the macrophage activation results. L. Sun and H. Cheng helped to draft the manuscript. All authors have read and approved the final manuscript.

## Conflict of interest

The authors declare that they have no conflicts of interest.

## Reference

Balachandran, P., Pugh, N. D., Ma, G., & Pasco, D. S. (2006). Toll-like receptor 2-dependent activation of monocytes by spirulina polysaccharide and its immune enhancing action in mice. *International Immunopharmacology, 6*(12), 1808-1814.

Cao, L., Li, R., Chen, X., Xue, Y., & Liu, D. (2016). Neougonin A Inhibits Lipopolysaccharide-Induced Inflammatory Responses via Downregulation of the NF-kB Signaling Pathway in RAW 264.7 Macrophages. *Inflammation, 39(6),* 1939-1948.

Carbonero, E. R., Gracher, A. H. P., Rosa, M. C. C., Torri, G., Sassaki, G. L., Gorin, P. A. J. &Iacomini, M. (2008). Unusual partially 3-O-methylated alpha-galactan from mushrooms of the genus Pleurotus. *Phytochemistry, 69(1)*:252-257.

Cho, S. M., Yun, B. S., Yoo, I. D. & Koshino, H. (2011). Structure of fomitellan A, a mannofucogalactan from the fruiting bodies of Fomitella fraxinea. *Bioorganic & Medicinal Chemistry Letters, 21(1)*:204-206.

Cianciulli, A., Calvello, R., Porro, C., Trotta, T., Salvatore, R., & Panaro, M. A. (2016). PI3K/Akt signalling pathway plays a crucial role in the anti-inflammatory effects of curcumin in LPS-activated microglia. *Int Immunopharmacol, 36,* 282-290.

Cui, F., Zan, X., Li, Y., Yang, Y., Sun, W., Zhou, Q., & Dong, Y. (2013). Purification and partial characterization of a novel anti-tumor glycoprotein from cultured mycelia of Grifola frondosa. *International Journal of Biological Macromolecules, 62,* 684–690.

Dubois, M., Gilles, K., Hamilton, J., Rebers, P., & Smith, F. (1951). A colorimetric method for the determination of sugars. *Nature, 168(4265),* 167-167.

Gordon, S. (2002). Pattern recognition receptors: doubling up for the innate immune response. *Cell, 111(7),* 927-930.

Han, S. B., Yoon, Y. D., Ahn, H. J., Lee, H. S., Lee, C. W., Yoon, W. K., Park, S. K., Kim, H. M. (2003). Toll-like receptor-mediated activation of b cells and macrophages by polysaccharide isolated from cell culture of acanthopanax senticosus. *International Immunopharmacology*, *3*(9), 1301-1312.

Han, X. Q., Li, W. J., Ko, C. H., Gao, X. M., Han, C. X. & Tu, P. F. (2013). Structure characterization and immunocompetence of a glucan from the fruiting bodies of Cantharellus cibarius. *Journal of Asian Natural Products Research, 15,* 1204-1209.

Ke, M., Wang, H., Zhang, M., Tian, Y., Wang, Y., Li, B., Yu, J., Dou, J., Xi, T., Zhou, C. (2014). The anti-lung cancer activity of sep is mediated by the activation and cytotoxicity of nk cells via tlr2/4 in vivo. *Biochemical Pharmacology*, *89*(1), 119-130.

Lemieszek, M. K., Nunes, F. M., Cardoso, C., Marques, G. & Rzeski, W. (2018). Neuroprotective properties of Cantharellus cibarius polysaccharide fractions in different in vitro models of

neurodegeneration. *Carbohydrate polymers, 197*,598-607.

Liana Inara de Jesusa, F. R. S., Lucimara M.C. Cordeiroa, Rilton A. de Freitasb, Leo J.L.D. Van Griensvenc, & Marcello Iacominia. (2018). Simple and effective purification approach to dissociate mixed waterinsoluble α- and β-D-glucans and its application on the medicinal mushroom Fomitopsis betulina. *Carbohydrate polymers, 200*, 353-360.

Meng, M., Cheng, D., Han, L., Chen, Y., & Wang, C. (2017). Isolation, purification, structural analysis and immunostimulatory activity of water-soluble polysaccharides from Grifola Frondosa fruiting body. *Carbohydrates Polymers, 157*, 1134–1143.

Meng, Y., Yan, J., Yang, G., Han, Z., Tai, G., Cheng, H., & Zhou, Y. (2018). Structural characterization and macrophage activation of a hetero-galactan isolated from Flammulina velutipes. *Carbohydrate Polymers, 183*, 207-218.

Needs, P., & Selvendran, R. (1993). Avoiding oxidative degradation during sodium hydroxide/methyl iodide-mediated carbohydrate methylation in dimethyl sulfoxide. *Carbohydrate research, 245*(1), 1-10.

Nowacka, N., Nowak, R., Drozd, M., Olech, M., Los, R., & Malm, A. (2014). Analysis of phenolic constituents, antiradical and antimicrobial activity of edible mushrooms growing wild in Poland. *LWT – Food Science and Technology, 59*, 689–694.

Nyman, A. A. T., Aachmann, F. L., Rise, F., Ballance, S. & Samuelsen, A. B. C. (2016). Structural characterization of a branched (1 → 6)- α-mannan and β-glucans isolated from the fruiting bodies of Cantharellus cibarius. *Carbohydrate Polymers, 146*, 197-207.

Rosado, F. R., Carbonero, E. R., Claudino, R. F., Tischer, C. A., Kemmelmeier, C., &Iacomini, M. (2003). The presence of partially 3-O-methylated mannogalactan from the fruit bodies of

edible basidiomycetes Pleurotus ostreatus “florida” Berk. And Pleurotus ostreatoroseus Sing. *FEMS Microbiology Letters, 221,* 119–124.

Ruthes, A. C., Smiderle, F. R., & Iacomini, M. (2016). Mushroom heteropolysaccharides: A review on their sources, structure and biological effects. *Carbohydrate Polymers, 136,* 358–375.

Ruthes, A. C., Rattmann, Y. D., Malquevicz-Paiva, S. M., Carbonero, E. R., Córdova, M. M., Baggio C. H., Santos A. R. S., Gorin P. A. J. &IacominiM. (2013). Agaricus bisporus fucogalactan: structural characterization and pharmacological approaches. *Carbohydrate Polymers, 92(1)*:184.

Sedmak, J. J., & Grossberg, S. E. (1977). A rapid, sensitive, and versatile assay for protein using Coomassie brilliant blue G250.*Analytical Biochemistry, 79*(1-2), 544-552.

Sweet, D. P., Albersheim, P., & Shapiro, R. H. (1975). Partially ethylated alditol acetates as derivatives for elucidation of the glycosyl linkage-composition of polysaccharides. *Carbohydrate Research, 40(2),* 199-216.

Takeuchi, O. & Akira S. (2010). Pattern Recognition Receptors and Inflammation. *Cell, 140,* 805-820.

Troll, J. V., Hamilton, M. L., Abel, M. L., Ganz, J., Bates, J. M., Stephens, W. Z., Melancon, E., Van der Varrt, M., Meijer, A. H., Distel, M., Eisen, J. S. & Guillenmin, K. (2018). Microbiota promote secretory cell determination in the intestinal epithelium by modulating host Notch signaling. *Development* **145**, dev155317.

Van den Bossche, J., O’Neill, L. A. & Menon, D. (2017). Macrophage immunometabolism: where are we (going)? *Trends in immunology. 38,* 395-406.

Villares, A., García-Lafuente, A., Guillamón, E.& Mateo-Vivaracho, L. (2013).Separation and characterization of the structural features of macromolecular carbohydrates from wild edible mushrooms. *Bioactive Carbohydrates and Dietary Fibre, 2*, 15–21.

Wang, H. T., Yang, L. C., Yu, H. C., Chen, M. L., Wang, H. J. & Lu, T. J. (2018). Characteristics of fucose-containing polysaccharides from submerged fermentation of Agaricus blazei Murill. *Journal of Drug Analysis, 26*,678-687.

Wang, H. X., Ngai, H. K. & Ng, T. B. (2003). A ubiquitin-like peptide with ribonuclease activity against various polyhomoribonucleotides from the yellow mushroom Cantharellus cibarius. *Peptides, 24*, 509-513.

Wasser, S. P. (2011). Current findings, future trends, and unsolved problems in studies of medicinal mushrooms. *Applied Microbiology and Biotechnology, 89*, 1323–1332.

Wasser, S. P. (2002). Medicinal mushrooms as a source of antitumor and immunomodulating polysaccharides. *Application of Microbiological Biotechnology, 60*, 258–274.

Yan, J., Han, Z., Qu, Y., Yao, C., Shen, D., Tai, G. & Zhou, Y. (2018). Structure elucidation and immunomodulatory activity of a beta-glucan derived from the fruiting bodies of Amillariella mellea. *Food Chemistry*, *240*, 534-543.

Yan, J., Meng, Y., Zhang, M., Cheng, H., Sun, L. & Zhou, Y. (2019). A 3-O-methylated heterogalactan from Pleurotus eryngii activates macrophages. *Carbohydrate Polymers, 206, 706-715*.

Zhang, A. Q., Xu, M., Fu, L. &Sun, P. L. (2013). Structural elucidation of a novel mannogalactan isolated from the fruiting bodies of Pleurotus geesteranus. *Carbohydrate Polymers*, 92(1):236-240.

Zhang, X., Yu, L., Bi, H., Li, X., Ni, W., Han, H., Tai, G. (2009). Total fractionation and characterization of the water-soluble polysaccharides isolated from Panax ginseng C. A. Meyer. *Carbohydrate Polymers*, *77*(3), 544-552.

Zhang, Y., Liu, Z., Ng, T. B., Chen, Z., Qiao, W., & Liu, F. (2014). Purification and characterization of a novel antitumor protein with antioxidant and deoxyribonuclease activity from edible mushroom Pholiota nameko. *Biochimie, 99,* 28–37.

Zhao, D. Q., Ding, X., Hou, Y. L., Hou, W. R., Liu, L., Xu, T. & Yang, D. N. (2018). Structural characterization, immune regulation and antioxidant activity of a new heteropolysaccharide from Cantharellus cibarius Fr. *Internation Journal of Molecular Medicine, 41,* 2744-2754.